Energy & Environmental Science

PAPER

View Article Online
View Journal

Thermochemical wastewater valorization via enhanced microbial toxicity tolerance†

Lahiru N. Jayakody[1], Christopher W. Johnson[1], Jason M. Whitham[2], Richard J. Giannone[2], Brenna A. Black[1], Nicholas S. Cleveland[1], Dawn M. Klingeman[2], William E. Michener[1], Jessica L. Olstad[1], Derek R. Vardon[1], Robert C. Brown[3], Steven D. Brown[2,4], Robert L. Hettich[2], Adam M. Guss[2], Gregg T. Beckham[1,*]

Abstract: Thermochemical (TC) biomass conversion processes such as pyrolysis and liquefaction generate considerable amounts of wastewater, which often contains highly toxic compounds that are incredibly challenging to convert via standard wastewater treatment approaches such as anaerobic digestion. These streams represent a cost for TC biorefineries, and a potential valorization opportunity, if effective conversion methods are developed. The primary challenge hindering microbial conversion of TC wastewater is toxicity. In this study, we employ a robust bacterium, *Pseudomonas putida*, with TC wastewater streams to demonstrate that aldehydes are the most inhibitory compounds in these streams. Proteomics, transcriptomics, and fluorescence-based immunoassays of *P. putida* grown in a representative wastewater stream indicate that stress results from protein damage, which we hypothesize is a primary toxicity mechanism. Constitutive overexpression of the chaperone genes, *groEL*, *groES*, and *clpB,* in a genome-reduced *P. putida* strain improves the tolerance towards multiple TC wastewater samples up to 200-fold. Moreover, the concentration ranges of TC wastewater are industrially-relevant for further bioprocess development for all wastewater streams examined here, representing different TC process configurations. Furthermore, we demonstrate proof-of-concept polyhydroxyalkanoate production from the usable carbon in an exemplary TC wastewater stream. Overall, this study demonstrates that protein quality control machinery and repair mechanisms can enable substantial gains in microbial tolerance to highly toxic substrates, including heterogeneous waste streams. When coupled to other metabolic engineering advances such as expanded substrate utilization and enhanced product accumulation, this study generally enables new strategies for biological conversion of highly-toxic, organic-rich wastewater via engineered aerobic monocultures or designer consortia.

Broader Context

Thermochemical biomass conversion represents a portfolio of promising technologies being developed for producing fuels and chemicals from lignocellulose. However, these processes invariably generate wastewater, which contains heterogeneous, toxic, and refractory compounds that are not converted during primary processing. These compounds are challenging for standard wastewater treatments, such as anaerobic digestion, due to their toxicity. This study presents a strategy to substantially increase the microbial toxicity tolerance to these streams, and thus potentially enables the use an aerobic, engineered monoculture or a designer consortia to funnel heterogeneous compounds in wastewater to valuable products. This strategy may enable valorization of streams that are both a cost and environmental burden to thermochemical biorefineries, and more generally to other industrial processes that generate organic-rich wastewater.

[1]*National Bioenergy Center, National Renewable Energy Laboratory, Golden, CO 80401, USA*
[2]*Oak Ridge National Laboratory, 1 Bethel Valley Rd, Oak Ridge, TN 37830, USA*
[3]*Bioeconomy Institute and Department of Mechanical Engineering, Iowa State University, Ames, IA 50011, USA*
[4]*LanzaTech, Inc., Skokie, IL 60077, USA*

* *Email: gregg.beckham@nrel.gov*

Pyrolysis | Thermochemical Conversion | Wastewater treatment | Chaperone | Polyhydroxyalkanoates

† Electronic supplementary information (ESI) available.

Introduction

Lignocellulosic biomass can enable the production of renewable fuels and chemicals, and will be an essential resource to mitigate climate change.[1] A diverse portfolio of biomass conversion technologies exist at varying stages of development from laboratory and pilot-scale, to several demonstration and industrial-scale processes around the world. Regardless of the process configuration, biomass conversion almost invariably generates wastewater containing dilute carbon and inorganic components, which typically are treated via standard wastewater approaches such as by combustion or oxidation to generate low-grade heat or anaerobic digestion (AD) to produce low-value biogas.[2-6] These waste streams are both a cost and a loss of potential high-value products for a biorefinery.[7-11]

Among thermochemical (TC) conversion processes, fast pyrolysis (FP) and catalytic fast pyrolysis (CFP) are promising options for production of biofuels and aromatic chemicals.[12-14] Pyrolysis relies on rapid heating of biomass in the absence of oxygen to generate either a bio-oil or vapor, both of which can be catalytically deoxygenated.[15] Several pioneer and demonstration plants employ pyrolysis, and research is being pursued to develop more robust catalysts and efficient processes to deoxygenate biomass-derived intermediates to fuels and aromatic compounds.[15] Additionally, pyrolysis streams may also have potential for co-feeding into petroleum refineries.[16] Given the oxygen content of biomass and the deoxygenation chemistry being pursued (which often employs dehydration), FP and CFP processes, like many processes that process organic chemicals, invariably generate wastewater containing un- or partially converted carbon that is slated for costly waste treatment processes.[7]

Recent characterization of TC wastewater streams from FP and CFP confirmed that the process configuration and conditions, biomass source, and catalyst impact the composition and carbon content of the resulting wastewater.[17] Refractory C1-C3 compounds such as glycolaldehyde (GA), acetate, and methanol along with partially deoxygenated aromatic compounds are prevalent, with total carbon content in some cases up to 350 g/L.[18] Given the toxic nature of these compounds and their high concentrations in multiple pyrolysis wastewater streams, it is highly likely that AD units will not be able to tolerate these streams without considerable *a priori* detoxification, supplementation with other biogenic carbon, and considerable dilution (>100-fold), as reported in previous studies attempting AD with pyrolysis wastewater.[19-24] Instead, most AD research focuses on applications to less toxic streams, such as municipal solid waste or food waste.

The concept of using microbial systems in concert with TC processes, however, has been pursued.[25-34] Most notably, Brown, Jarboe, Wen, Chen, and others have pioneered the concept of using microbes to convert pyrolysis-derived substrates to value-added compounds. These approaches generally target the isolation of single substrates or narrow classes of compounds (e.g., levoglucosan), which are extensively purified and detoxified. Using these separated, detoxified streams, downstream microbial conversion can be achieved. Separations and purification are often the most expensive steps in a bioprocess, and accordingly, being able to avoid detoxification and purification to narrow libraries of compounds would be ideal to combine the beneficial attributes of TC processing with microbial conversion.[35]

In this study, we originally were motivated to valorize the toxic, heterogeneous mixtures of organic compounds in pyrolysis wastewater to value-added co-products. To accomplish this task biologically without detoxification and fractionation will likely require microbes or designer communities engineered to exhibit unprecedented toxicity tolerance, very broad substrate specificity, and the ability to produce value-added compounds. The most substantial, enabling challenge to accomplish this objective is overcoming toxicity, as compounds including aldehydes, ketones, phenolics, and acids are commonly found in TC wastewater streams.[18] These molecules often exhibit severe microbial toxicity via damage to biomolecules or membranes, disruption of metabolic circuits, creation of redox cofactor imbalances, and/or depletion of ATP generation.[36-40] More broadly, organic-rich wastewater streams are produced from both biomass processing and organic chemical manufacturing, and microbial biotechnology solutions to valorize these streams are receiving more attention.[41, 42] To date, most solutions still rely on AD using a microbial consortium, which limits the product spectrum that can be targeted and sets an upper threshold on the stream toxicity, but the ability to employ an engineered microbe or designer consortium with extremely high toxicity tolerance and substrate specificity could enable the production of a broad range of valuable products.

In the past few decades, multiple biological strategies have emerged to overcome microbial toxicity associated with substrates and end-products, including evolution and engineering.[40, 43, 44] Systems biology-enabled screening has identified genetic targets that enable *in situ* detoxification of multiple toxic compounds, and enzyme engineering, re-wiring metabolic circuits, and redox cofactor engineering can further improve detoxification.[45-48] In addition, membrane, efflux, transporter, and DNA repair machinery engineering have been identified as viable targets to protect cells.[40, 49, 50] Notably, engineering post-translational protein machineries of biocatalysts is a vital tool for enhancing tolerance of microorganisms.[51-56] For instance, bacterial tolerance to high temperature and solvents such as ethanol, butanol, and 1, 2, 4-butanetriol has been achieved by engineering chaperones, or heat shock proteins (Hsp) that provide protein "quality control", including re-folding, ensuring correct functional confirmation, disaggregation of protein aggregates, protein trafficking, and degradation of misfolded or damaged proteins.[54, 57-59]

Chaperones execute their functions via allosteric machinery, energized by cycles of ATP binding and hydrolysis.[59, 60] Chaperones are categorized as Hsp10, Hsp20, Hsp40, Hsp60, Hsp70, Hsp90, and Hsp100, based on their molecular weights in kDa, and exhibit broad substrate specificity.[58] For instance, the bacterial GroESL complex, consisting of the Hsp60 chaperonin, GroEL, and its Hsp10 co-chaperone, GroES, functions to refold numerous proteins.[61] Like the GroESL complex, the Hsp70 chaperonin, DnaK, complexes with the co-chaperones Hsp40, DnaJ, and Hsp20, GrpE, to form DnaJKE, which is crucial for the survival of bacteria under stress conditions.[62] The Hsp100 chaperone, including the bacterial ClpA, ClpB, and ClpX are referred to as unfoldases and disaggregases. ClpA and ClpX promote specific protein degradation via the ClpP protease, while ClpB disassembles protein aggregates and refolds them into functional proteins together with the DnaJKE and/or the GroESL system.[58, 63, 64]

In this work, we report a multi-omics investigation of the biological toxicity mechanisms relevant to upgrading TC wastewater streams with the robust soil bacterium *Pseudomonas putida* KT2440.[65] This strain was chosen given its well-characterized robustness to toxic compounds, its broad catabolic repertoire, and its ability to survive and thrive in harsh environments.[65, 66] We first dissect the chemical toxicity of an

exemplary TC waste stream and show that aldehydes are the most toxic components to *P. putida* KT2440. We then deploy transcriptomics (RNA-seq), proteomics, and green fluorescence protein (GFP)-based immunoassays to demonstrate that protein damage is a key component of TC wastewater toxicity. Using this information, we show that overexpression of the chaperone genes *clpB*, *groES*, and *groEL* enables *P. putida* KT2440 to overcome the acute toxicity of multiple TC wastewater streams from pilot-scale operations. As an initial proof-of-concept, we demonstrate that the engineered *P. putida* strain can utilize a fraction of the waste carbon at an industrially process-relevant substrate concentration as its sole source of carbon and energy.[67, 68] Overall, this study highlights the potential for using an engineered, aerobic monoculture for TC wastewater valorization by overcoming the key technical challenge of substrate toxicity, a strategy that can be broadly applied for strain development.

Results

Baseline toxicity of TC waste streams to *P. putida* KT2440

Several exemplary TC wastewater streams from FP and CFP pilot-scale processes were evaluated for their baseline toxicity to *P. putida* KT2440 (**ESI Fig. S1**). The most toxic wastewater stream is from a FP-with-fractionation (FPF) process.[18, 69] This stream is lethal at a concentration of 0.1% (v/v), which translates to 0.34 g/L of organic carbon (**Fig. 1A**). We envisioned that developing a *P. putida* KT2440 strain tolerant to the FPF stream could be a base strain for other TC wastewater streams. From our previous work, compounds in the FPF stream were identified and quantified to a mass closure of 80% (**ESI Table S1**).[18] Using these data, a synthetic FPF mixture was formulated (**ESI Table S1**) with the 32 most abundant compounds present in FPF, and this stream accurately captures the FPF toxicity to *P. putida* (**Fig. 1B**, R^2=0.99). The compounds present in the FPF stream were classified according to chemical functionality, aldehydes, ketones, phenolics, or acids, and the growth rate of *P. putida* was evaluated against each class of compounds (**Fig. 1C).** Of the functional group classes, aldehydes are the predominant contributor of FPF toxicity ($p < 0.05$), ketones and phenols have minor effects ($p < 0.05$), and acids do not contribute to toxicity, at least at the concentration tested here ($p>0.05$). Given that combinational effects of these different functional groups may contribute to the total FPF toxicity, a fractional factorial experiment was performed, followed by partial least square (PLS) modeling to characterize the individual contributions of the functional groups to the total toxicity of the FPF stream (**ESI Fig. S2**). The variable important parameter (VIP) score of the functional groups, an indicator of the contribution of individual parameters to the total effect, confirmed that aldehydes are critical to the combinational toxicity of the FPF stream, followed by acids, phenols, and ketones (**Fig. 1D**). We also individually analyzed the EC_{50} values (the effective concentration that decreases the growth rate by 50%) for the 32 most abundant compounds (**ESI Table S2**). The results reveal that formaldehyde and glycolaldehyde (GA) have low EC_{50} values (~2 mM) for *P. putida* compared to those of ketones, phenols, and acids. Overall, these results demonstrate that aldehydes are the main contributors to the FPF stream toxicity, suggesting that alleviating aldehyde toxicity could contribute to the development of a strain tolerant to TC wastewater streams.

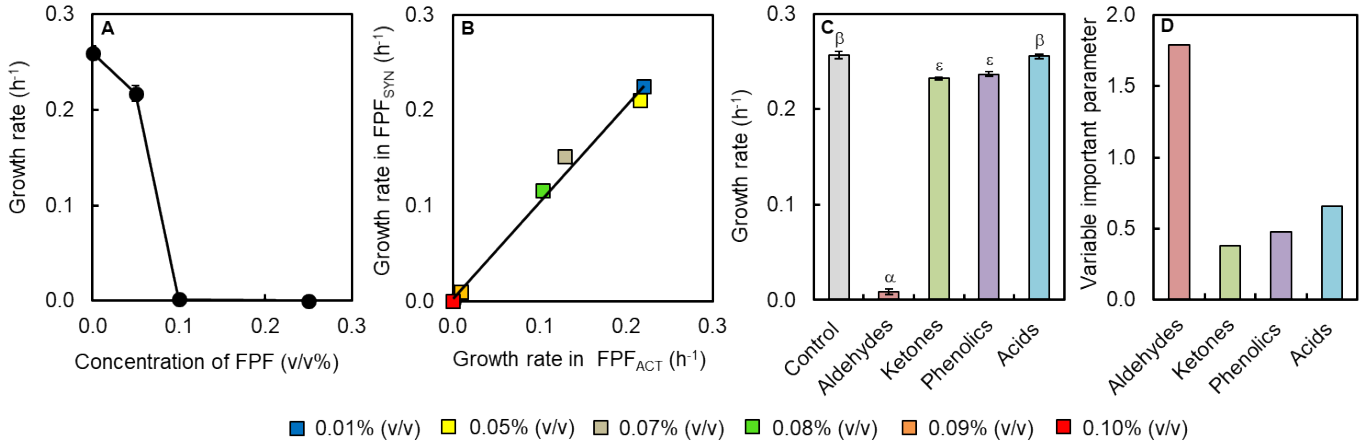

Figure 1. Baseline toxicity of FPF stream component to toxicity with *P. putida* KT2440. (A) Growth rate of *P. putida* in the FPF stream as a function of dilution factor. (B) Growth rates of *P. putida* KT2440 in M9 medium containing 20 mM glucose and different concentration of synthetic FPF (FPF_{SYN}) or actual FPF (FPF_{ACT}). (C) The effect of functional group classes in the FPF stream on the growth of *P. putida* in minimal (M9) media containing 20 mM glucose. The medium was supplemented with a combination of compounds belonging to the functional groups at the same concentration found in a 0.1% (v/v) dilution of the FPF stream, which is a lethal concentration to *P. putida* KT2440. (D) Contribution of different functional groups to the toxicity of the FPF stream on *P. putida* KT2440. Results are expressed as means ± SEM (n=3). Bars labeled with different symbols (α, β, ε) indicate statistical significance of the functional groups ($p < 0.05$; one-way ANOVA followed by Tukey's post hoc honest significance difference test). Bars labeled with the same symbol indicate no statistically significant difference ($p > 0.05$). FPF: fast pyrolysis with-fractionation.

Elucidation of the mechanism of FPF toxicity

To identify the molecular mechanism of the FPF stream toxicity to *P. putida* KT2440 and identify rational genetic targets to enhance its tolerance, RNA-seq transcriptomics and proteomics analyses were performed under FPF-induced stress. The same analyses were conducted with a single toxic aldehyde. Specifically, GA is a ubiquitous compound found in TC wastewater streams (3 mM-850 mM), and FPF contains 785 mM of GA.[18] Hence, it was selected as a model aldehyde for parallel multi-omics analysis. In the RNA-seq analysis, 43% of highly up-regulated and 44% of down-regulated genes in FPF-treated cells are in common with GA-treated cells (**Fig. 2A**). The genes that are significantly up-regulated in *P. putida* KT2440 in both GA and FPF-treatments (**ESI Table S3**) suggest that the microbe may convert inhibitory aldehydes including GA into less toxic acids/alcohols by inducing expression of dehydrogenases (PP_2426, PP_2476, PP_3621, PP_3622, PP_3623, PP_3745, PP_3746, and PP_3747), export the inhibitory compounds by upregulating transporters and efflux pumps (PP_3425, PP_3426, PP_3427, and PP_2647), and/or alter its cell envelope (PP_2213 and PP_3519). Gene ontology (GO) enrichment analysis reveals low representation of the energy and core metabolism categories including ATP synthesis, succinate-CoA ligase (ADP formation), and nitrogen-metal bond-forming complex coordination, which is consistent with decreased growth after treatment with the FPF stream compared to control cultures (**ESI Table S4**). Enrichment in iron binding and siderophore transport GO terms upon GA treatment may be a response to demand for Fe-S cofactors for the upregulated glycolate oxidase (PP_3747), coproporphyrinogen III oxidase (PP_4264), and a protein annotated as Fe-S cluster-binding (PP_4259). The glycolate oxidase encoded by *glcDEF* (PP_3745, PP_3746, and PP_3747) is responsible for detoxifying GA to the less toxic glyoxylic acid via glycolic acids.[70] In addition, there was an enrichment of genes with the GO term for ribosome structural constituents in GA-treated cells, suggesting that GA disrupts translational machinery.

In parallel to RNAseq analysis, we performed proteomics to detect the stress response of *P. putida* KT2440 at the level of translation. The results reveal that many proteins are significantly different in abundance in response to GA stress (151 proteins increased in abundance, $N.\log_2 > 1$, $p < 0.05$; 218 proteins reduced in abundance $N.\log_2 < -1$, $p < 0.05$) and FPF (319 proteins increased in abundance, $N.\log_2 > 1$, $p < 0.05$; 403 proteins decreased in abundance $N.\log_2 < -1$, $p < 0.05$) (**ESI Fig. S3**). In agreement with GO enrichment analysis of differentially expressed genes, we detected similar enrichment of GO-terms for proteins significantly reduced in abundance after FPF treatment (**ESI Table S5**). Interestingly, we found a disparity between transcription and translation in FPF-treated cells. Several proteins were significantly reduced in abundance after FPF treatment, although the gene expression was highly upregulated ($N.\log_2 > 1$, $p < 0.05$) (**ESI Table S6**), including PP_0149; AapP, PP_1300; TctC, PP_1418; AsnB, PP_1750; TetR, PP_2475; PP_3610; PP_3332; HemN, PP_4264; and PP_5391 ($\log_2 < -1$, $p < 0.05$). None of these proteins exhibit a secretion signal peptide according to SignalP 4.1.[71] *Ab initio* prediction of non-classical protein secretion using SecretomeP 2.0 Server was only positive with PP_5391.[71, 72] These results suggest that these proteins are subject to post-transcriptional or post-translational regulation or may have been damaged in FPF-treated cells, but that differences in protein and mRNA abundance are not likely attributed to secretion.

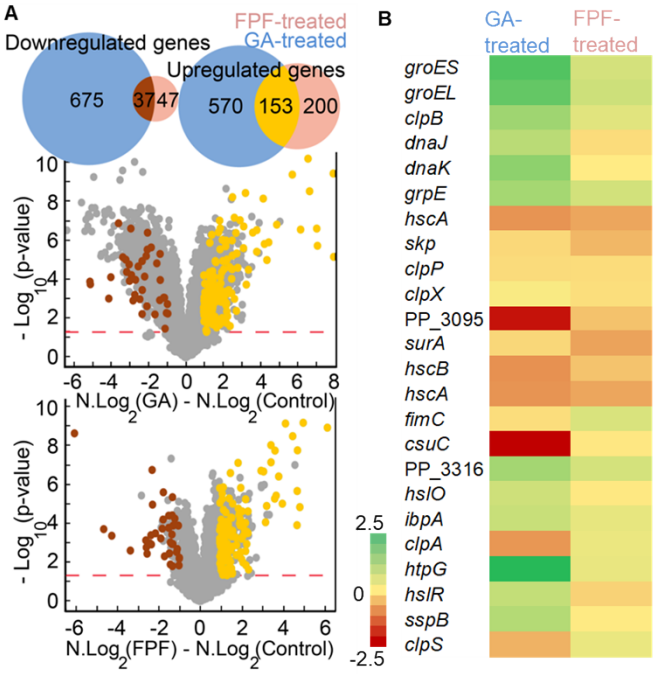

Figure 2. Highlights of global transcriptional profiles of the strains under GA or FPF-induced stress. (A) A volcano plot of RNA-seq profiles of *P. putida* KT2440 up-regulated and down-regulated genes under GA or FPF-treated cells relative to the untreated cells. Genes commonly up- (Normalize base 2 logarithm [$N.\log_2$] ≥ 1, $p < 0.05$) or down-regulated ($N.\log_2 \leq 1$, $p < 0.05$) under GA- or FPF-treated conditions relative to control cells are denoted in pale orange and maroon dots, respectively. (B) Heat map of the $N.\log_2$ value of *P. putida* KT2440 chaperone genes up- or down-regulated under GA or FPF treatment. GA: glycolaldehyde, FPF: fast pyrolysis with-fractionation.

It has been well documented that aldehydes, the key toxic component of the FPF stream, impose molecular toxicity via protein damage.[73] Indeed, GA, the major aldehyde present in FPF is a well-known post-translational protein-damaging agent.[74, 75] To demonstrate the *in vivo* effect of GA and FPF in this system, a GFP-expressing strain of *P. putida* KT2440 was cultured in medium supplemented with GA (2 mM), FPF (0.05% (v/v)), or un-supplemented. Cell-free extract from these conditions was immunoblotted to detect the presence of GFP. In GA or FPF-treated cells, we observed a band around 37 kDa (*vide infra*), suggesting a cross-linking of GFP (28 kDa) with and an unidentified protein of around 10 kDa. GA or FPF-treated cells also exhibit significantly lower free-GFP levels compared to the untreated cells (46.8% in GA-treated cells and 18.1% in FPF-treated cells relative to the untreated controls). Furthermore, GFP inclusion bodies formed in cells treated with GA or FPF, which might be due to misfolding[76, 77] or cross-linking of the GFP protein (**ESI Fig. S4**). FACS analysis revealed that GA or FPF-treated cells have a weaker GFP signal relative to the control (*vide infra*). Together, these results suggest that FPF may be crosslinking and/or causing

misfolding of GFP. Although, the category was not enriched in GO ontologies analysis, we found that several chaperone proteins, which are responsible for turnover and refolding of damaged proteins, including *clpB, groES, groEL, dnaK, dnaJ, grpE,* and *htpG* were among the most highly expressed genes under the GA or FPF treatment (**Fig. 2B**). Collectively, these results suggest that protein damage is a key contributor of FPF toxicity. Thus, we hypothesized that overexpression of chaperones to rescue damaged or misfolded proteins would enhance the tolerance of *P. putida* to FPF.

The effect of targeted expression of chaperones on *P. putida* tolerance to FPF

We targeted two major protein recovery chaperone machineries, DnaJKE and GroESL, to improve the tolerance of *P. putida* to FPF (**ESI Fig. S5A**). Given that protein cross-linking is potentially critical as well, we also evaluated the protein disaggregating chaperone, ClpB. We first constructed plasmids to overexpress combinations of these chaperone genes, and investigated tolerance of *P. putida* KT2440 containing these plasmids to GA and FPF. We found that co-expression of *clpB*, *groES,* and *groEL* chaperones had a supra-additive effect on improving the tolerance of *P. putida* KT2440 to FPF (**Fig. 3**), and an additive effect on tolerance to GA (**ESI Fig. S5B**) relative to the overexpression of those chaperone genes alone or all other combinations ($p < 0.05$).

Based on these results, we developed a more industrially applicable strain that overexpresses these genes without the use of plasmids. To accomplish this, we integrated a second copy of the native *clpB, groES,* and *groEL* chaperone genes into the genome of *P. putida* KT2440 at intergenic site between PP_1584 and PP_1585 (**ESI Fig. S6**). The *tac* promoter, which is a strong, constitutive promoter in *P. putida* KT2440, was included to drive expression of these genes.[78, 79] We then tested the tolerance of this strain, LJ014, to increasing concentrations of the 32 most abundant compounds in the TC wastewater streams[18] and found that the strain exhibits tolerance to higher concentrations of 30 of these relative to wild-type *P. putida* KT2440, except 2-methylcylopentenone and 2-oxobutanol (**Fig. 4**). These include aldehydes (vanillin by 7.5-fold and GA by 1.5-fold), ketones (2-butenolide or 3-methyle-2-butenolide by 1.5-fold), acids (acrylic acid by 3.5-fold and butyric acid by 2.5-fold), phenolics (guaiacol by 3.5-fold and *m*-cresol by 3.5-fold), and to the prevalent alcohol, methanol (by 1.5-fold). Since we achieved enhanced tolerance to the majority of compounds present in the TC wastewater streams analyzed here, we next characterized the performance of LJ014 in FPF.

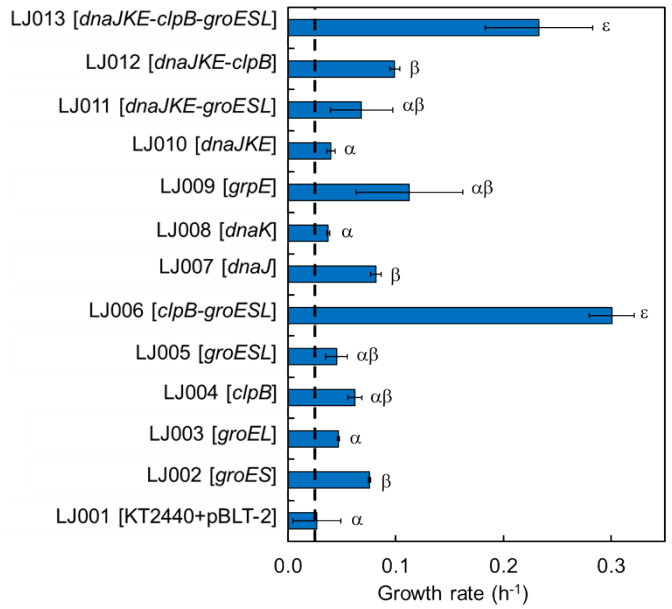

Figure 3. Growth rates of plasmid based chaperones-expressing *P. putida* KT2440 strains in FPF. Growth assays were performed in M9 medium containing 20 mM glucose supplemented with 0.075% (v/v) FPF. *groESL*: *groES* and *groEL*, and *dnaJKE*: *dnaJ, dnaK*, and *grpE*. The results are expressed as means ± SEM (n=3). Bars labeled with different symbols (α, β, and ε) indicate statistical significance in the differences in growth rate between those strains ($p < 0.05$; one-way ANOVA followed by Tukey's post hoc honest significance difference test). Bars labeled with the same symbol indicate no statistically significant difference ($p > 0.05$). FPF: fast pyrolysis with-fractionation, ANOVA: analysis of variance.

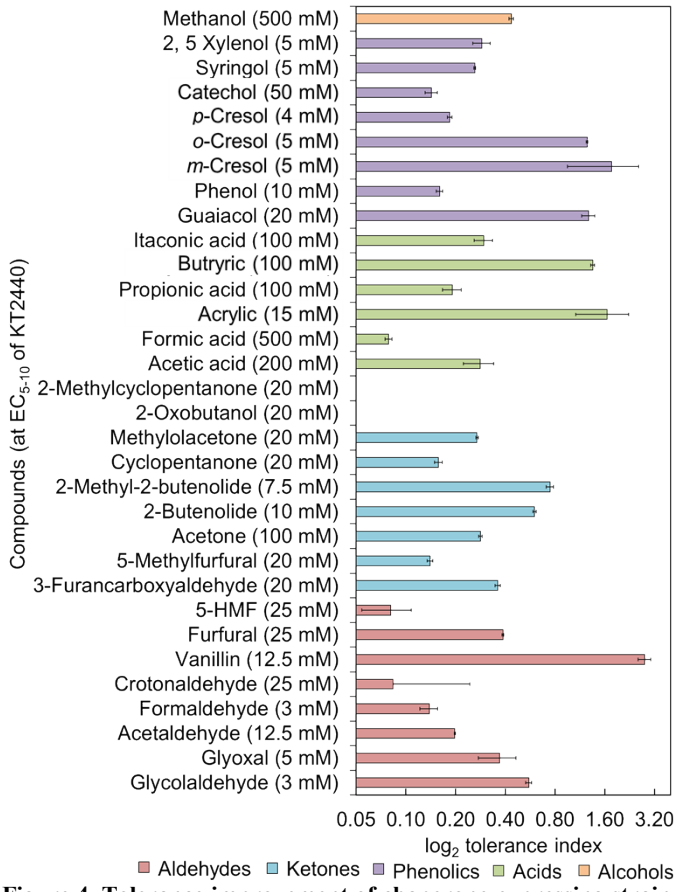

Figure 4. Tolerance improvement of chaperone-expressing strain LJ014 to the major compounds found in the TC wastewater streams. The tolerance index is defined as ratio of maximum tolerable concentration of LJ014 (*clpB:groES:groEL*) and KT2440.

Survival and protein recovery of the strain co-expressing GroESL and ClpB exposed to FPF

To evaluate the viability of the GroESL and ClpB overexpression strain, LJ014, and wild-type *P. putida* KT2440, we treated the cells with 1% (v/v) FPF and performed fluorescence-based live/dead cell viability assays, which differentially label live and dead cells, and evaluated these

populations via fluorescence-activated cell sorting (FACS). LJ014 exhibits high cell viability after 12 h of FPF treatment relative to KT2440 (82.9±7.5-fold higher, $p < 0.01$) (**Fig. 5A**). Parallel colony-forming assays revealed that only LJ014 formed colonies on LB plates after 12 h exposure to FPF (**Fig. 5B**). These data clearly demonstrate that strong, constitutive co-expression of the chaperones genes *clpB, groES,* and *groEL* markedly improves the cell viability and growth of *P. putida* KT2440 exposed to FPF.

We next monitored the fate of GFP in the LJ014 strain after treatment with FPF. ImageJ analysis of immunoblot (Fig. 5C) band intensity revealed that the free GFP level was significantly higher in the GPF-expressing LJ014 relative to the GFP-expressing wild-type *P. putida* KT2440 after 3 h of FPF treatment (48.2% vs 18.5% relative to free GFP of untreated controls). Consistent with a larger amount of free GFP, the GFP-expressing LJ014 cells exhibit a 3-fold higher GFP fluorescent signal compared to that of the GFP-expressing wild-type strain when exposed to FPF **(Fig. 5D)**. Overall, these results demonstrate that the chaperone over-expression strain, LJ014, strain is capable of producing a larger amount of functional GFP relative to *P. putida* KT2440 in the FPF stream.

Overexpression of chaperone genes *groESL* and *clpB* alters the global proteomic profile of *P. putida* KT2440

We next evaluated changes to the global proteomic profile of LJ014. Proteomes of treated and untreated LJ014 and KT2440 were distinct on the PLS plot (**ESI Fig. S7**). In the absence of any treatment, the overexpression of *clpB*, *groES*, and *groEL* in LJ0114 resulted in increased abundance of 76 proteins ($N.\log_2 > 1, p < 0.05$) and decreased abundance of 169 proteins ($N.\log_2 < 1, p < 0.05$) relative to KT2440 (**ESI Fig. S8A**). DnaJKE and HscB (a co-chaperone of maturation pathway of Fe–S proteins), and the chaperone assisting ATPase protein encoded by PP_3316 (**ESI Fig. S8B**), were among the proteins with the greatest abundance in LJ014 relative to KT2440. It has been reported that the stoichiometry of chaperones greatly affects the overall efficiency of the system[54, 80], so increased abundance of these other chaperones may have been a response to overexpression of ClpB, GroES, and GroEL in LJ014, such that the entire chaperone cascade might be tuned appropriately. However, GO enrichment analysis did not identify any GO categories among the proteins that were differentially expressed between the LJ014 and KT2440 grown in M9 medium containing 20 mM glucose. As shown in **ESI Fig. S7**, the samples from LJ014 and KT2440 treated with FPF were also distantly clustered in the PLS analysis plot, reflecting a difference in their global proteomic profiles. When grown in the presence of the FPF stream, we found that siderophore and ion binding proteins GO categories were enriched in the LJ014 strain relative to the KT2440 wild-type (**ESI Table S5**). LJ014 had 206 proteins that were increased in abundance relative to the KT2440 strain in M9 medium containing FPF ($N.\log_2 > 1$, $p < 0.05$) (**ESI Table S7**), some of which could contribute to its enhanced tolerance. Increased protein expression of chaperones ClpB, GroES, and GroEL also resulted in increased in abundance of proteins involved in universal stress response (PP_2130), redox cofactor biosynthesis (UbiG, PP_1765; Dxr, PP_1597; GrxC, PP_5054, GloB, PP_4144) detoxification of toxic compounds (YeaE, PP_3120; PP_3248; Ttg2E, PP_0962; PP_3671), DNA repair (MutY, PP_0286; Ung, PP_1413; RecC, PP_4674), RNA processing (RnpA, PP_0008), membrane stability (OpgH, PP_5025), regulation of protein synthesis and ribosomal stability (RsfS, PP_4809), and central metabolism (ZwfB, PP_4042; GlpD, PP_1073). Notably, several proteins that were significantly reduced in abundance despite being highly expressed at transcriptional level in KT2440 treated with FPF, as reported above, were highly abundant in FPF-treated LJ014 cells. These included, PP_ 0837 ($N.\log_2 = 2.22$, $p = 0.022$); TetR, PP_ 1387 ($N.\log_2 = 1.17$, $p = 0.014$); TctC, PP_1418 ($N.\log_2 = 1.47$, $p = 0.009$); PP_1503 ($N.\log_2 = 8.29$, $p = 0.001$); AsnB, PP_1750 ($N.\log_2 = 5.29$, $p = 0.004$); PP_2059 ($N.\log_2 = 4.39$, $p = 0.013$); PP_3332 ($N.\log_2 = 2.6$, $p = 0.0321$); PP_3610 ($\log_2 = 1.72$, $p = 0.014$); Gad, PP_4281 ($N.\log_2 = 1.54$, $p = 0.002$); PP_4738 ($N.\log_2 = 4.95$, $p = 0.000$); and PP_5391 ($N.\log_2 = 3.35$, $p = 0.001$). These results indicate that overexpression of GroESL and ClpB leads to greater abundance of proteins associated with other cellular defense machineries, and suggests the recovery of protein biosynthesis (translation, folding, and/or solubility) under FPF stress, leading to an overall more robust cellular defense.

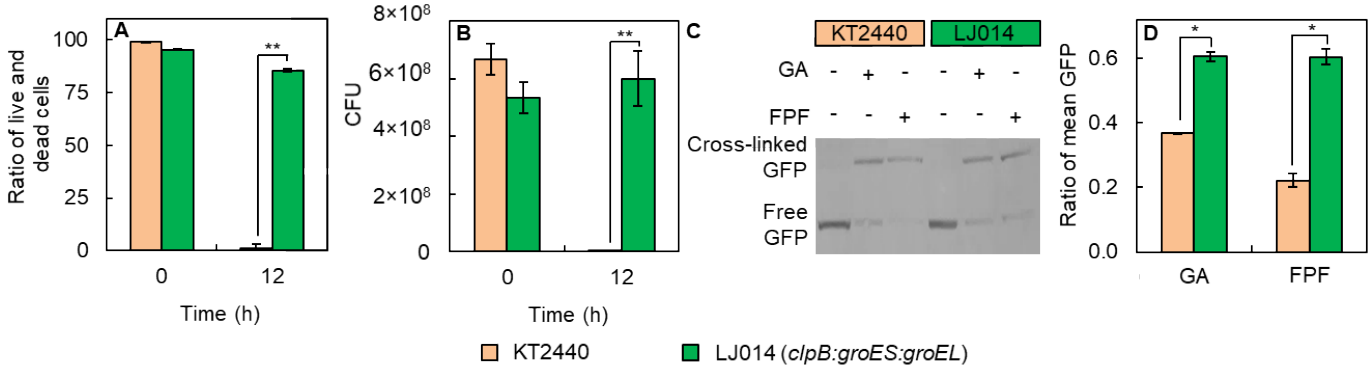

Figure 5. Cell viability and protein recovery by the engineered LJ014 strain. (A) live and dead cell assay under 1 % (v/v) FPF treatment. (B) Colony forming capability of survival 1 % (v/v) FPF-treated cells. (C) Western blot (WB) analysis of GFP protein recovery by engineered strain. (D) FACS analysis of GFP showing the ratio of mean GFP frequency of treated and untreated samples. The level of statistical significance is indicated for differences between the two strains (* $p < 0.05$, ** $p < 0.01$). CFU: colony forming unit , GA: glycolaldehyde, FPF: fast pyrolysis with-fractionation GFP: green fluorescent protein.

Bioconversion of the FPF stream using LJ014

The next question was whether the engineered LJ014 strain could use FPF as a sole carbon and energy source. To this end, we grew the LJ014 strain in 50 mL of M9 medium containing 1% FPF (v/v), which is equivalent to 3.44 g/L of organic carbon as a sole carbon source in a shake flask. We observed that the LJ014 survived and grew using FPF carbon, but the KT2440 strain did not (**Fig. 6A**). HPLC analysis showed that acetate and GA are the major carbon components consumed within 24 h by LJ014 (**ESI Fig. S9**). LJ014 used 52.27±1.12% of total carbon in FPF by the end of the cultivation at 72 h, while KT2440 was unable to utilize carbon in FPF (**Fig. 6B**). Of note, based on descriptions in published literature, native *P. putida* KT2440 metabolism theoretically allows complete conversion of 45.25% (e.g. acetic, formic, propionic, vanillin, and catechol) of carbon present in FPF for growth and energy and partial metabolism of 18.62% (e.g. glycolaldehyde, furfural, 5-HMF) (ESI Table S1). Thus, LJ014 converted approximately 82% of theoretically accessible carbon in the FPF medium within 72 h.

We next tested the capability of the LJ014 strain to convert FPF waste-carbon into medium-chain-length polyhydroxyalkanoates (*mcl*-PHAs), biopolymers with potential as biodegradable plastics and chemical precursors. *P. putida* natively accumulates *mcl*-PHAs as a carbon and energy reserve via intermediates of fatty acid biosynthesis and degradation under the condition of a nutrient limitation and excess carbon.[81, 82] The composition and yield of *mcl*-PHAs vary depending on the substrate and metabolic and physiologic state of the cell.[67, 82, 83] To induce production of *mcl*-PHAs, we grew the cells in nitrogen-limited M9 medium supplemented with 1% (v/v) FPF. *mcl*-PHA accumulation was observed microscopically (**Fig. 6E**), and quantitative analysis revealed that the LJ014 strain accumulated mcl-PHAs around 0.7% of dry cell weight **(Fig. 6C)**, which accounted for a yield of 0.42±0.04 g *mcl*-PHAs per liter of FPF. As expected in *P. putida* KT2440, the *mcl*-PHA profiles are mainly of chain lengths 10 and 12, with some 8-carbon chain-length *mcl*-PHA detected in the samples, but below the quantification range (**Fig. 6D**). Based on the growth and carbon analysis, these results show that expression of *groES*, *groEL*, and *clpB* enabled *P. putida* to metabolize available carbon by partially overcoming the FPF stream toxicity.

***groESL* and *clpB* overexpression leads to improved *P. putida* EM42 tolerance to multiple TC wastewater streams**

Given that the chaperone-dependent machinery has a high ATP demand, we hypothesized that the *P. putida* EM42, a reduced-genome strain of *P. putida* KT2440 that has a 1.6-fold higher ATP content and 1.2-fold higher adenylate energy charge relative to KT2440 due to the deletion of the flagellar machinery, could provide further improvements.[84, 85] Of note, the EC_{50} value of FPF on the EM42 strain is 0.1% (v/v), a 2-fold tolerance improvement over the parental KT2440 strain (data not shown). Thus, we developed the strain LJ015 by integrating an extra copy of *tac* promotor-driven chaperone genes *clpB, groES*, and *groEL* into the *P. putida* EM42 genome rather than the KT2440 genome as with LJ014.

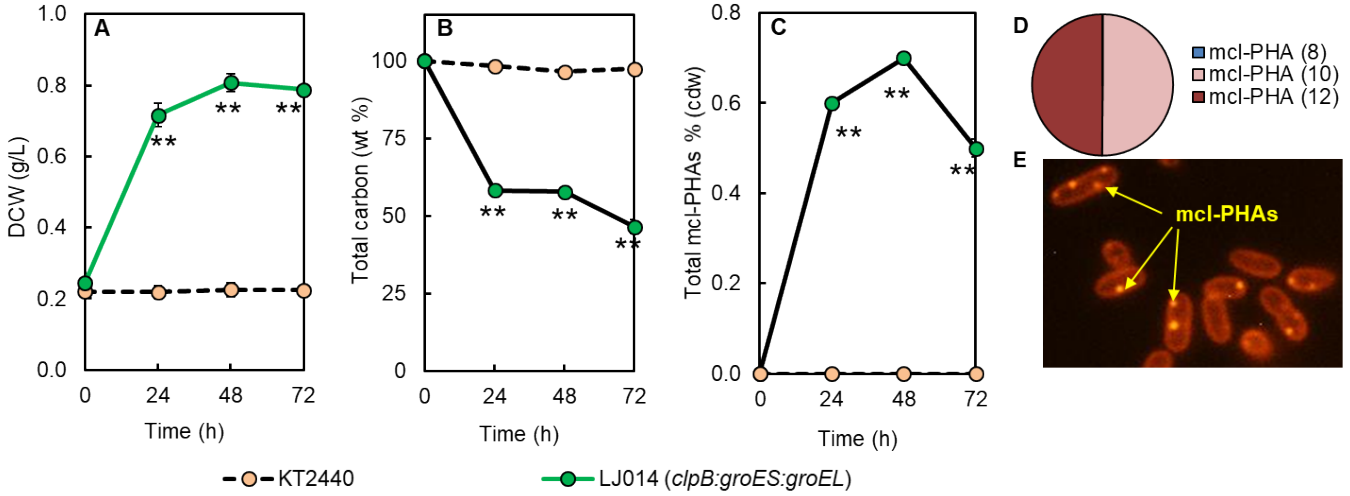

Figure 6. The chaperone overexpression strain LJ014 uses waste carbon in the FPF stream for growth, energy and *mcl*-PHA production. (A) Growth profile of strains in the FPF as a sole carbon source. (B) Total carbon utilization of the strains. (C) Conversion of FPF carbon into *mcl*-PHA by the engineered strain. (D) Composition of *mcl*-PHAs. (E) Nile-red staining of mcl-PHA molecules. The results are expressed as means ± SEM (n=3). The level of statistical significance is indicated for differences between the two strains (**p <0.01). DCW: dry cell weight, mcl-PHAs: medium-chain-length polyhydroxyalkanoates

LJ015 substantially improved the cell survival and colony forming capability under FPF stress (**ESI Fig. S10**). The maximum tolerable FPF concentration of the LJ014 and LJ015 strains are 2.5% and 10% (v/v), respectively. Thus, LJ015 exhibits 4-fold tolerance improvement over LJ014 to FPF, and the overall tolerance of LJ015 to FPF is improved by 200-fold relative to the KT2440 (**Fig. 7**). The FPF stream represents only one pyrolysis-derived wastewater stream, and as we demonstrated in a previous study, the waste stream composition depends significantly on the upstream process configuration.[18] To determine the general applicability of this chaperone overexpression strategy, we evaluated the LJ015 strain tolerance to TC waste streams from FP, *ex-situ* CPF, and *in-situ* CFP, all of which were previously characterized.[18] In M9 medium containing these TC waste streams, LJ015 exhibits substantially higher cell survival than KT2440, with the

number of colony-forming units 5% (v/v) greater when cells were exposed to FP, 50% (v/v) greater for those exposed to *in-situ* CFP, and 5% (v/v) greater when exposed to *ex-situ* CFP (**ESI Fig. S10**). These results reflect the remarkable tolerance improvements of LJ015 to TC wastewater streams (**Fig. 7A**). Its enhanced tolerance enables LJ015 to access >12 g/L of carbon in all classes of TC wastewater streams, an industrially-relevant concentration of carbon that could be used in a fed-batch cultivation process for valorizing these waste carbon streams. This would otherwise be impossible with the wild-type *P. putida* strain, which is already known for its stress tolerance (**Fig. 7B**).[86-88] LJ015 can thus serve as a base chassis for engineering strains for valorization of process-specific TC wastewater streams.

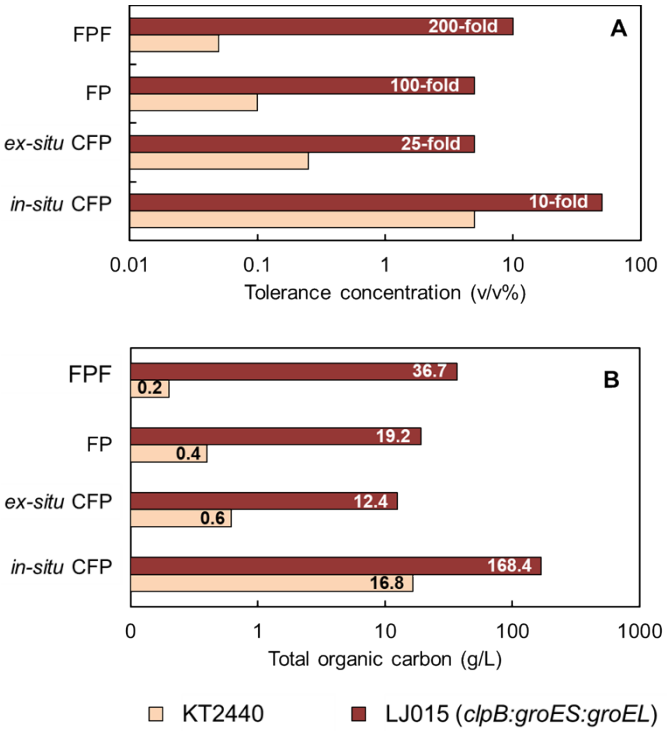

Figure 7. Tolerance thresholds of the engineered chaperone-overexpressing *P. putida* EM42 strain (LJ015) to different TC wastewater streams. (A) Maximum tolerable concentration of the strains was defined as the concentration which at least 1% of live cells are accounted in FACS analysis and enabling to form colonies after 12 h in 5 mL culture of 20 mM glucose-containing M9 medium supplemented with different concentration of various TC wastewater streams. Initial OD_{600} of samples were kept at 1. The tolerance improvement of the engineered strain over the wild-type strain is presented as folds change. (B) Total organic carbon in different TC wastewater streams of the strains at their maximum tolerable concentration. FP: fast pyrolysis, FPF: fast pyrolysis with-fractionation, CFP: catalytic fast pyrolysis.

Discussion

In this study, we demonstrate that overexpression of the autologous chaperone genes *clpB*, *groES*, and *groEL*, which encode primary elements of stress defense, is a partial solution to overcome the chemical stress of TC wastewater streams (**Fig. 8**). The LJ015 strain enables access to industrially-relevant levels of carbon in the four classes of TC wastewater streams tested. Going forward, this is a major step towards an industrially-relevant biological strategy to valorize TC wastewater without substantial *a priori* detoxification. Specifically, this base strain can enable production of high value products via metabolic engineering aimed at both expanding substrate utilization and improving and targeting product formation.

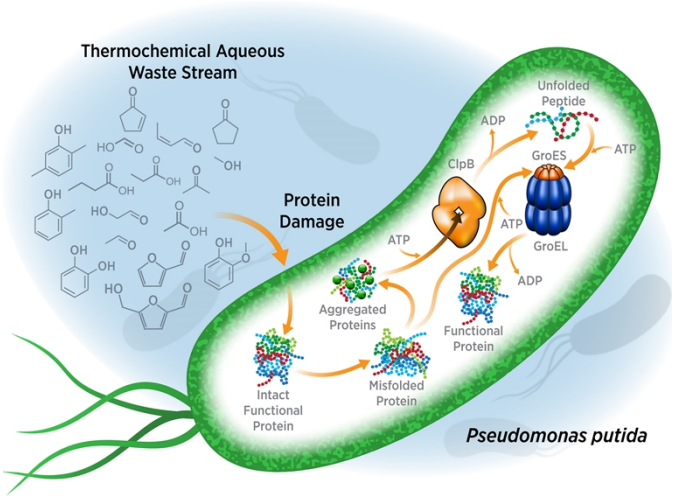

Figure 8. Illustration of the chaperone-dependent tolerance mechanism of *P. putida* to thermochemical wastewater streams. Protein damage generated by the components of thermochemical wastewater streams results in protein misfolding and aggregation. Disaggregation by ClpB and re-folding by the GroES and GroEL complex restores protein functionality. Overexpression of the ClpB, GroES, and GroEL chaperones in the engineered *P. putida* strains described here enhance this process and improve tolerance to thermochemical wastewater streams. ATP: adenosine triphosphate, ADP: adenosine diphosphate.

Conventional solutions to cleanup of organic-rich, highly-toxic wastewater streams from TC biorefineries, and more generally from organic chemical manufacturing, primarily employ strategies such as catalytic hydrothermal gasification, which can produce methane and carbon dioxide.[89, 90] AD to produce methane is another commonly employed strategy, but stream toxicity is a major barrier to its use, essentially precluding its utility for TC biorefineries.[19-24] Given how little research has been done in this space, wastewater treatment has been identified as a major uncertainty in the development of TC processes.[11] Designer biological systems that employ aerobic catabolic pathways could potentially enable the production of higher-value compounds than methane. Importantly, rigorous techno-economic analysis will be necessary to compare the biological strategy proposed here to more standard approaches for detoxification of TC wastewater streams, such as catalytic hydrothermal gasification and AD, which we will report in a future study. [89, 90]

Previous efforts have employed chaperones to overcome end-product toxicity.[44, 53, 54, 57] For example, Zingaro and coworkers demonstrated the overexpression of native *Escherichia coli groESL-clpB* genes conferred solvent tolerance to end-product alcohols such as ethanol and butanol.[54] Here, we show that constitutive expression of the native *P. putida* KT2440 GroESL-ClpB chaperone system is effective for improving the tolerance of the strain toward a broader range of toxic

compounds containing aldehyde, ketone, phenolic, and acid functional groups (**Fig. 4**), as well as the combinatorial chemical toxicity found in TC wastewater streams. The chemical compounds tested in this study are often found in lignocellulosic hydrolysates and other industrial wastewater streams, including those generated during the production of second-generation biofuels are known to be quite toxic.[37, 74, 91] Thus, the approach developed here could also be broadly utilized in different biorefinery scenarios as a strain engineering strategy to overcome substrate toxicity, which goes beyond the current applications of chaperones for improving tolerance of microbes toward end-product inhibition or temperature stress.[44, 54-57, 92, 93] Moreover, the GroESL-ClpB chaperone system might be further optimized by overexpressing partner chaperones such as *hscB* or novel candidate partner proteins identified in the global proteomics profile of the LJ014 strain (e.g., uncharacterized proteins). Fine-tuning the expression level of the chaperones to maintain their overall and relative concentrations as appropriate to the stream toxicity could increase the overall efficiency of this ATP-intensive system as reported earlier.[54, 79, 94] We intend to pursue these strategies in future work.

Protein damage is a key component of aldehyde toxicity.[73] The extent of damage is closely related to the electrophilic activity (ω) and chemical structure of aldehydes. Short aliphatic aldehydes such as formaldehyde and acetaldehyde target neutrophilic lysine residues on proteins, and form carboxyl-methyl lysine (CML).[73] Beyond the CML formation, the most toxic subclass of aldehyde, α-hydroxyaldehydes such as GA, cross-link proteins by targeting neutrophilic lysine residues and cysteine residues via the formation of Schiff-base and concurrent Amadori rearrangement, which leads to re-generation of the aldehyde carbonyl group after the first attack on a protein, forming a second covalent bond with a different protein **(ESI Fig. S11**). Previous work has shown *in vitro* formation of GA-mediated crosslinked glutathione.[73, 74] In this study, we observed the *in vivo* formation of cross-linked GFP in *P. putida* KT2440 under GA or FPF stress (**Fig. 5C**). In addition to the remarkable ability of ClpB to rescue stress-damaged proteins via ATP-driven mechanical unfolding of aggregated proteins, our GFP WB results suggest that the chaperone ClpB might be able to rescue the GA-mediated cross-linked proteins by breaking the cross-links *in vivo* (**Fig. 5C**).[62, 95] However, further structural and biochemical studies are required to understand the mechanism of disaggregating chemically crosslinked proteins by ClpB. Of note, our study as well as several previous reports emphasize that deploying metabolic engineering strategies to alleviate aldehyde toxicity is able to overcome chemical stress by a substantial margin.[46, 51, 91, 96]

Multi-omics analyses (**ESI Table 3**) reported here highlight additional engineering targets for enhanced *P. putida* tolerance to TC wastewater including the efflux pumps MexEF and OprN, the alcohol dehydrogenase PP_ 2476, and hypothetical protein PP_3770. Overexpression of these autologous genes shows enhanced tolerance to aldehydes and FPF (data not shown). These particular genes are under further investigation to understand their mechanisms and substrate specificity, and will be incorporated into the LJ015 strain to further enhance tolerance in a future study. Additionally, several functionally unknown genes were upregulated in GA- or FPF-treated conditions and warrant further studies to identify their role(s) in bacterial tolerance and conversion of toxic substances (**ESI Tables 3, 5, 6**). Accordingly, these multi-omics data are a rich source for identifying new genetic traits to further improve strain tolerance to different chemical functional groups.

Microbial tolerance to chemical stressors is multigenic and complex.[45, 46] To that end, we observed that the *clpB-groESL* gene expression triggers the recovery of proteins of the key stress response pathways including detoxification, transporters and efflux pumps, DNA repair, membrane integrity, and transcriptional regulators. Induction of such proteins suggest that toxicity goes beyond protein damage. While we did not investigate toxic effects to other cellular macromolecules besides proteins, α-hydroxyaldehydes are known to impose direct DNA and RNA glycation, concurrent DNA mutation, DNA strand breaks, and cytotoxicity.[97-99] The enhancements made to the LJ015 strain seem to alleviate these toxic effects, by increasing expression of nucleotide repair proteins including adenine glycosylase MutY and uracil-DNA glycosylase Ung.[100, 101] This observation suggests cross-talk between the ClpB-GroESL chaperones and DNA repair systems. Crosstalk between post-translational protein machineries during DNA damage response is well established in eukaryotes.[102-104] If (and how) ClpB and GroESL coordinate stress-related protein expression in *P. putida* requires further investigation.

A two-pronged system against chemical toxicity, namely detoxification and cell protection, is known to provide enhanced strain robustness.[49, 51, 105] Accordingly, our ultimate objective is to engineer metabolic routes to convert toxic compounds in TC wastewater streams, while protecting the cellular macromolecules via the damage-repair machineries of *P. putida*. To this end, we have previously engineered *P. putida* KT2440 to efficiently utilize GA, furfural, HMF, and levoglucosan.[33, 106, 107] Several promising autologous and heterologous pathways have also been identified for metabolism of acetone, acetaldehyde, formate, methanol, phenol, and cresol in *P. putida* as well.[108, 109] Stacking these pathways into LJ015 could enable utilization of nearly 100% of carbon present in the TC wastewater streams, an endeavor we are currently pursuing.

Lastly, several metabolic engineering strategies have been adopted to enhance *mcl*-PHAs production in *P. putida,* and these approaches will be leveraged to improve *mcl*-PHA production in the LJ015 strain.[110-112] Beyond *mcl*-PHA production, engineering the aromatic catabolic pathways in LJ015 could enable conversion of the aromatic carbon in the TC wastewater stream (e.g., which is rich in the *ex-situ* CFP stream) for the production of atom-efficient, high-value building blocks such as muconic acid.[113-116] Given the chemical heterogeneity of TC wastewater streams, techno-economic analysis coupled with metabolic modeling will be useful for identifying ideal product(s) based on specific TC wastewater streams and aid in predicting which metabolic routes will require tailoring to optimize conversion.

Conclusion

In this study, we have shown that overexpression of chaperone genes *clpB-groESL* can be used to overcome the acute chemical toxicity of TC wastewater streams in the metabolically versatile bacterium *P. putida*. By overcoming a primary challenge in TC wastewater valorization, this work demonstrates the potential for complete utilization of waste carbon present in TC wastewater streams to produce value-added chemicals. Valorization of this waste carbon could ultimately provide an economic benefit to TC biorefineries.

Materials and methods

Strains, media, and chemicals

P. putida strains used in this study are listed in **ESI Table S8**. Chemically competent NEB 5-alpha F'Iq *E. coli* (New England Biolabs, USA) was used for the plasmid manipulations. *E. coli* was grown in Luria-Bertani (LB) medium (Lennox) containing 10 g/L tryptone, 5 g/L yeast extract, and 5 g/L NaCl, in the presence of 50 µg/mL kanamycin. LB plates containing 50 µg/mL kanamycin were prepared by adding 15 g/L agar to LB media, and used to select plasmid bearing *E. coli* and *P. putida* strains. *P. putida* strains were grown in modified M9 minimal medium (M9) containing 6.78 g/L Na_2HPO_4, 3.00 g/L K_2HPO_4, 0.50 g/L NaCl, 1.66 g/L NH_4Cl, 0.24 g/L $MgSO_4$, 0.01g/L $CaCl_2$, and 0.002g/L $FeSO_4$, supplemented with 3.60 g/L glucose and/or different concentrations of TC wastewater streams neutralized (pH 7) with NaOH. For analysis of *mcl*-PHA production, N-limiting M9 medium was prepared by substituting 0.24 g/L g/L NH_4Cl with 0.132 g/L of $(NH_4)_2SO_4$. All the chemicals used for the study were obtained from Sigma-Aldrich (St. Louis, MO, USA). TC wastewater streams used for the study are listed in **ESI Table S9**. FPF synthetic medium (FPF-syn) was prepared by adding the 32 most abundant compounds present in FPF at concentrations equal to those found in actual FPF (**ESI Table S1**). FPF synthetic-aldehyde, -ketones, -phenolics, and -acids media were prepared by adding subsets of those 32 compounds based on their functional groups.

Plasmid construction

Amplicons were obtained from *P. putida* KT2440 genomic DNA by performing polymerase chain reactions (PCR) with primers (**ESI Table S10)** synthesized by Integrated DNA Technologies (IDT) and Phusion® High-Fidelity PCR Master Mix with HF Buffer (New England Biolabs, USA). Plasmids were constructed using NEBuilder® HiFi DNA Assembly (New England Biolabs) according to the manufacturer's instructions. The vector, pBLT-2 (Addgene plasmid # 22806) was used for plasmid-based overexpression of genes.[117] A derivative of the plasmid pK18mobsacB (ATCC 87097), constructed to exclude the mobilization factor and other extraneous DNA and named pK18sB, was used for construction of the plasmid for genome integration of the chaperone genes (**ESI Fig. S12**, **ESI Table S11**).[118] Plasmids were transformed into NEB 5-alpha F'Iq *E. coli* according to the manufacturer's instructions. Transformants were selected on LB (Lennox) plate supplemented with 50 µg/mL kanamycin grown at 37°C. Correct assembly was confirmed by restriction enzymes digestion and the sequences of all plasmid inserts were confirmed by Sanger sequencing (GENEWIZ, Inc., USA). Further descriptions about specific plasmid construction can be found in **ESI Table S12**.

Strain construction

For plasmid-based gene expression, *P. putida* KT2440 was transformed by electroporation as previously described and selected on LB plates containing 50 µg/mL kanamycin.[119]

Genomic integration of the *tac* promoter-driven chaperone genes, (*clpB, groES*, and *groEL*) in *P. putida* KT2440 (LJ014) and *P. putida* EM42 (LJ015) was accomplished using the antibiotic-*sacB* system of selection and counter-selection.[120] A detailed description of the method, with modifications for *P. putida* KT2440, can be found in Johnson and Beckham, 2015.[121] Following sucrose selection, single colonies were subjected to colony PCR with primers oLJ154 (Fwd) and oLJ155 (Rev) to identify those with genome integration of the chaperone genes.

Growth assay and fermentation analysis

Toxicity of the TC wastewater streams and toxic compounds present in FPS were evaluated in microplate growth assays performed in a Bioscreen C MBR analyzer (Growth Curves US, Piscataway, NJ). Pre-cultures of the strains were prepared by inoculating 25 mL M9 medium supplemented with 20 mM glucose in a 125 mL baffled flask to an OD_{600} of 0.05-0.1 and incubating shaking at 225 rpm, 30°C. At mid log phase (OD_{600} 0.5-1.0) cells were harvested by centrifugation at 13,000 rpm, and the cell pellets were washed twice and resuspended in M9 medium without a carbon source. These resuspended cells were used to inoculate microplate wells containing 200 µL of M9 medium supplemented with 20 mM glucose and various concentrations of TC wastewater streams or their components to OD_{600} 0.1. Microplates were then incubated at 30°C with maximum shaking and growth was measured by reading the absorbance ($OD_{420\text{-}580}$) every 30 min. Growth rates were calculated according to the growth curve equation.[122] Combinational inhibition assay analysis of the functional groups present in FPF are included in ESI material and methods.

To assess the growth and carbon utilization of the strains in FPF, shake flask experiments were performed using 125 mL baffled flasks containing 50 mL modified M9 media supplemented with 1% (v/v) FPF (pH 7) and inoculated to OD_{600} 0.2 with cells prepared as above but resuspended in M9 medium containing 1% (v/v) FPF. Cultures were incubated shaking at 225 rpm, 30 °C. 2 mL samples were collected periodically and subjected to HPLC analysis (ESI-material and methods), total carbon analysis (ESI materials and methods), and OD_{600} growth measurement using a Beckman DU640 spectrophotometer (Beckman Coulter, Brea CA). The dry cell weight (DCW) of the cultures was calculated based on the OD_{600} to DCW conversion equation [CDW (g/L) = 0.5746 (OD_{600} of sample)].[114]

Proteomics and RNAseq analysis

Cells treated with GA or FPF or left untreated were collected for analysis at mid-log phase. Details of sample preparation and analysis are included in the ESI Material and Methods.

Quantification *mcl*-PHA production from FPF carbon

To quantify *mcl*-PHAs as a percent of the dry cell weight in cultures growth in media containing FPF, shake-flask experiments were performed in N-limiting media as described above. *mcl*-PHA quantification is described in ESI materials and methods.

Microscopic observation of *P. putida*

Microscopic observation of mcl-PHAs in *P. putida* by epifluorescence, was performed by removing 1 mL from FPF-containing shake flask cultures after 48 h. Cells were pelleted by centrifugation at 13,000 rpm for 1 min, washed twice with 1X phosphate buffer saline (PBS), resuspended in 1 mL PBS-containing 10 µg/mL Nile Red (Molecular probes, Invitrogen Cooperation, USA), and incubated at room temperature in the dark for 30 min. Cells were pelleted again, washed with 1X PBS, and resuspended in 1 mL PBS. 5 µL of resuspended cells were mixed with 5 µL of 1% (w/v) low-melting-temperature agarose to immobilize the cells, and placed on a microscopic slide with coverslip. Nile Red fluorescence was observed with band-pass filtering between 560-590 nm using a Nikon Eclipse 80i microscope (Nikon cooperation, Japan)**.**

Fluorescence-activated cell sorting (FACS) analysis

Live and dead cell counts were determined using the LIVE/DEAD™ BacLight™ Bacterial Viability Kit (ThermoFisher Scientific, USA) according to the manufacture's instructions. Briefly, 1 mL samples were collected periodically, and culture supernatant was discarded after centrifugation at 13,000 rpm for 1 min. Cell pellets were washed twice with 0.85% (w/v) NaCl, and resuspended in 1mL 0.85% (w/v) NaCl solution for staining. 1.5 µL each of component A (SYTO 9) and component B (Propidium Iodide) was added to the samples and incubated at room temperature in the dark for 15 min. Samples were centrifuged at 13,000 rpm for 1 min and the supernatant was discarded. Cell pellets were washed with 0.85% (w/v) NaCl solution and resuspended in BD FACSFlow™ sheath fluid (BD Biosciences, USA) for analysis. Live and dead cells counts were monitored using a BD FACSAria™ (BD Biosciences, USA) instrument equipped with BD FACSDiva data acquisition and analytical software. The 488 nm laser coupled with B530-30A (530 nm) and B610-20A (610 nm) detection channels were used to sort the green (live) and red (dead) fluorescent cells, respectively. For each sample 30,000 events were recorded to generate scatter plots of B530-30A and B610-20A, which were used to determine the number of live and dead cells based on live and dead population regions assigned based on live and dead controls. For monitoring GFP protein fluorescence, samples were excited at 488 nm and detected at 530 nm and 20,000 events were recorded to generate each histogram.

Statistical analysis

All experiments were performed in triplicate or greater as indicated in figure legends. Results are expressed as the mean value and error bars represent the standard error of the mean (SEM). For a pair-wise comparison of the differences between the sample averages of two groups, a one-tailed Student's t-test without known deviations was employed.[123] A one-way analysis of variance (ANOVA) followed by Tukey's post hoc honest significance difference test was used for several comparisons.[124] Data analysis was performed using KaleidaGraph statistical program (Synergy Software, PA, USA). The Partial Least Square (PLS) regression modeling of multivariate data were performed with XLSTAT software (Addinsoft, USA). Fisher's Exact statistical test was performed with differentially expressed gene and protein datasets to identify enriched GO-terms compared to GO-terms of the entire *Psudomonas putida* KT2440 genome determined by the standard workflow of Blast2GO 4.1. [123]

Conflicts of Interest

LJ and GTB have filed a patent application on the strains described in this manuscript.

Acknowledgements

The NREL authors thank the U.S. Department of Energy Bioenergy Technologies Office (DOE-BETO) for funding this work via Contract No. DE-AC36-08GO28308. JMW, RJG, SDB, RLH, AMG, and GTB acknowledge funding for the multi-omics efforts by the BioEnergy Science (BESC) and the Center for Bioenergy Innovation (CBI), both U.S. Department of Energy Bioenergy Research Centers supported by the Office of Biological and Environmental Research in the DOE Office of Science. Oak Ridge National Laboratory is managed by UT-Battelle, LLC, for the U.S. DOE under contract DE-AC05-00OR22725. Transcriptomics data were generated by the U.S. Department of Energy Joint Genome Institute, a DOE Office of Science User Facility, supported by the Office of Science of the U.S. Department of Energy under Contract No. DE-AC02-05CH11231. We thank Mary Biddy, Abhijit Dutta, Christopher Kinchin, Josh Schaidle, and other NREL colleagues for helpful conversations regarding pyrolysis wastewater and Anna Knapp, Payal Khanna, and Emily Fulk for their assistance in constructing the pK18sB vector. We David Dayton at RTI International for providing pyrolysis-derived wastewater streams. The U.S. Government retains and the publisher, by accepting the article for publication, acknowledges that the U.S. Government retains a nonexclusive, paid up, irrevocable, worldwide license to publish or reproduce the published form of this work, or allow others to do so, for U.S. Government purposes.

References

1. A. J. Ragauskas, C. K. Williams, B. H. Davison, G. Britovsek, J. Cairney, C. A. Eckert, W. J. Frederick, J. P. Hallett, D. J. Leak and C. L. Liotta, *Science*, 2006, **311**, 484-489.
2. L. R. Lynd, M. S. Laser, D. Bransby, B. E. Dale, B. Davison, R. Hamilton, M. Himmel, M. Keller, J. D. McMillan, J. Sheehan and C. E. Wyman, *Nature Biotechnol.*, 2008, **26**, 169.
3. P. R. Gogate and A. B. Pandit, *Adv. Environ. Res.*, 2004, **8**, 501-551.
4. P. R. Gogate and A. B. Pandit, *Adv. Environ. Res.*, 2004, **8**, 553-597.
5. M. A. Oturan and J.-J. Aaron, *Crit. Rev. Env. Sci. Technol.*, 2014, **44**, 2577-2641.
6. L. Appels, J. Lauwers, J. Degrève, L. Helsen, B. Lievens, K. Willems, J. Van Impe and R. Dewil, *Renew. Sust. Energy Rev.*, 2011, **15**, 4295-4301.
7. A. Dutta, A. Sahir, E. Tan, D. Humbird, L. J. Snowden-Swan, P. Meyer, J. Ross, D. Sexton, R. Yap and J. Lukas, *Process Design and Economics for the*

Conversion of Lignocellulosic Biomass to Hydrocarbon Fuels: Thermochemical Research Pathways with In Situ and Ex Situ Upgrading of Fast Pyrolysis Vapors, National Renewable Energy Laboratory, Golden, CO, 2015.
8. R. Davis, L. Tao, C. Scarlata, E. C. D. Tan, J. Ross, J. Lukas and D. Sexton, *Process Design and Economics for the Conversion of Lignocellulosic Biomass to Hydrocarbons: Dilute-Acid and Enzymatic Deconstruction of Biomass to Sugars and Catalytic Conversion of Sugars to Hydrocarbons*, NREL, Golden, CO, 2015.
9. R. Davis, L. Tao, E. Tan, M. J. Biddy, G. T. Beckham, C. Scarlata, J. Jacobson, K. Cafferty, J. Ross, J. Lukas, D. Knorr and P. Schoen, *Process Design and Economics for the Conversion of Lignocellulosic Biomass to Hydrocarbons: Dilute-Acid Prehydrolysis and Enzymatic Hydrolysis Deconstruction of Biomass to Sugars and Biological Conversion of Sugars to Hydrocarbons*, NREL, Golden, CO, 2013.
10. M. J. Biddy, R. Davis, D. Humbird, L. Tao, N. Dowe, M. T. Guarnieri, J. G. Linger, E. M. Karp, D. Salvachúa, D. R. Vardon and G. T. Beckham, *ACS Sustain. Chem. Eng.*, 2016, **4**, 3196-3211.
11. M. J. Biddy, A. Dutta, S. Jones and A. Meyer, *Ex-Situ Catalytic Fast Pyrolysis Technology Pathway*, National Renewable Energy Laboratory, Golden, CO, 2013.
12. S. Yaman, *Energy Convers. Manag*, 2004, **45**, 651-671.
13. T. R. Carlson, G. A. Tompsett, W. C. Conner and G. W. Huber, *Top. Catal.*, 2009, **52**, 241.
14. R. French and S. Czernik, *Fuel Process. Technol.*, 2010, **91**, 25-32.
15. D. A. Ruddy, J. A. Schaidle, J. R. Ferrell III, J. Wang, L. Moens and J. E. Hensley, *Green Chem.*, 2014, **16**, 454-490.
16. M. S. Talmadge, R. M. Baldwin, M. J. Biddy, R. L. McCormick, G. T. Beckham, G. A. Ferguson, S. Czernik, K. A. Magrini-Bair, T. D. Foust and P. D. Metelski, *Green Chem.*, 2014, **16**, 407-453.
17. A. K. Starace, B. A. Black, D. D. Lee, E. C. Palmiotti, K. A. Orton, W. E. Michener, J. ten Dam, M. J. Watson, G. T. Beckham and K. A. Magrini, *ACS SUSTAIN. CHEM. ENG.*, 2017, **5**, 11761-11769.
18. B. A. Black, W. E. Michener, K. J. Ramirez, M. J. Biddy, B. C. Knott, M. W. Jarvis, J. Olstad, O. D. Mante, D. C. Dayton and G. T. Beckham, *ACS SUSTAIN. CHEM. ENG.*, 2016, **4**, 6815-6827.
19. P. M. Fedorak and S. E. Hrudey, *Water Res.*, 1984, **18**, 361-367.
20. C. Torri and D. Fabbri, *Bioresour. Technol.*, 2014, **172**, 335-341.
21. T. Willner, P. Scherer, D. Meier and W. Vanselow, *Chem. Ing. Tech.*, 2004, **76**, 838-842.
22. V. Andreoni, P. Bonfanti, D. Daffonchio, C. Sorlini and M. Villa, *Biol. Waste*, 1990, **34**, 203-214.
23. T. Hübner and J. Mumme, *Bioresour. Technol.*, 2015, **183**, 86-92.
24. D. Fabbri and C. Torri, *Curr. Opin. Biotechnol.*, 2016, **38**, 167-173.
25. L. R. Jarboe, Z. Wen, D. Choi and R. C. Brown, *Appl. Microbiol. Biotechnol.*, 2011, **91**, 1519.
26. Y. Shen, L. Jarboe, R. Brown and Z. Wen, *Biotechnol. Adv.*, 2015, **33**, 1799-1813.
27. J. Lian, S. Chen, S. Zhou, Z. Wang, J. O'Fallon, C.-Z. Li and M. Garcia-Perez, *Bioresour. Technol.*, 2010, **101**, 9688-9699.
28. J. Lian, M. Garcia-Perez and S. Chen, *Bioresour. Technol.*, 2013, **133**, 183-189.
29. J. Lian, M. Garcia-Perez, R. Coates, H. Wu and S. Chen, *Bioresour. Technol.*, 2012, **118**, 177-186.
30. Z. Chi, M. Rover, E. Jun, M. Deaton, P. Johnston, R. C. Brown, Z. Wen and L. R. Jarboe, *Bioresour. Technol.*, 2013, **150**, 220-227.
31. M. R. Rover, P. A. Johnston, T. Jin, R. G. Smith, R. C. Brown and L. Jarboe, *ChemSusChem*, 2014, **7**, 1662-1668.
32. D. S. Layton, A. Ajjarapu, D. W. Choi and L. R. Jarboe, *Bioresour. Technol.*, 2011, **102**, 8318-8322.
33. J. G. Linger, S. E. Hobdey, M. A. Franden, E. M. Fulk and G. T. Beckham, *Metab. Eng. Commun.*, 2016, **3**, 24-29.
34. X. Zhao, Z. Chi, M. Rover, R. Brown, L. Jarboe and Z. Wen, *Environ. Prog. Sustain. Energy.*, 2013, **32**, 955-961.
35. A. J. J. Straathof, in *Comprehensive Biotechnology*, Academic Press, Burlington, 2nd edn., 2011, pp. 811-814.
36. L. N. Jayakody, N. Hayashi and H. Kitagaki, *Material and process for energy: communicating current research and technological development. Formatex Research Center, Badajox, Spain*, 2013, 302-311.
37. E. Palmqvist and B. Hahn-Hägerdal, *Bioresour. Technol.*, 2000, **74**, 25-33.
38. J. Sikkema, J. De Bont and B. Poolman, *Microbiol. Rev.*, 1995, **59**, 201-222.
39. T. Y. Mills, N. R. Sandoval and R. T. Gill, *Biotechnol Biofuels.*, 2009, **2**, 26.
40. S. A. Nicolaou, S. M. Gaida and E. T. Papoutsakis, *Metabolic engineering*, 2010, **12**, 307-331.
41. L. T. Angenent, K. Karim, M. H. Al-Dahhan, B. A. Wrenn and R. Domíguez-Espinosa, *Trends Biotechnol.*, 2004, **22**, 477-485.
42. P. H. Nielsen, *Microbial biotechnol.*, 2017, **10**, 1102-1105.
43. M. J. Dunlop, *Biotechnol Biofuels.*, 2011, **4**, 32.
44. A. Mukhopadhyay, *Trends Microbiol.*, 2015, **23**, 498-508.
45. J. R. Almeida, T. Modig, A. Petersson, B. Hähn‐Hägerdal, G. Lidén and M. F. Gorwa‐Grauslund, *J. Chem. Technol. Biotechnol.*, 2007, **82**, 340-349.
46. Z. L. Liu, *Appl. Microbiol. Biotechnol.*, 2011, **90**, 809-825.
47. T. U. Chae, S. Y. Choi, J. W. Kim, Y.-S. Ko and S. Y. Lee, *Curr. Opin. Biotechnol.*, 2017, **47**, 67-82.
48. T.-M. Lo, W. S. Teo, H. Ling, B. Chen, A. Kang and M. W. Chang, *Biotechnol. Adv.*, 2013, **31**, 903-914.
49. F. A. Dingler and K. J. Patel, *Science*, 2017, **357**, 130-131.
50. Z. Tan, P. Khakbaz, Y. Chen, J. Lombardo, J. M. Yoon, J. V. Shanks, J. B. Klauda and L. R. Jarboe, *Metab. Eng.*, 2017, **44**, 1-12.
51. L. N. Jayakody, M. Kadowaki, K. Tsuge, K. Horie, A. Suzuki, N. Hayashi and H. Kitagaki, *Appl. Microbiol. Biotechnol.*, 2015, **99**, 501-515.
52. H. Xiao and H. Zhao, *Biotechnol Biofuels.*, 2014, **7**, 78.
53. E. T. Papoutsakis, *Curr. Opin. Biotechnol.*, 2008, **19**, 420-429.
54. K. A. Zingaro and E. T. Papoutsakis, *Mbio*, 2012, **3**, e00308-00312.
55. G. Luan, H. Dong, T. Zhang, Z. Lin, Y. Zhang, Y. Li and Z. Cai, *J. Bacteriol.*, 2014, **178**, 38-40.

56. D. Fiocco, V. Capozzi, P. Goffin, P. Hols and G. Spano, *Appl. Microbiol. Biotechnol.*, 2007, **77**, 909-915.
57. K. A. Zingaro and E. T. Papoutsakis, *Metab. Eng.*, 2013, **15**, 196-205.
58. H. Saibil, *Nat. Rev. Mol. Cell Biol.*, 2013, **14**, 630.
59. K. Richter, M. Haslbeck and J. Buchner, *Mol. Cell*, 2010, **40**, 253-266.
60. Y. E. Kim, M. S. Hipp, A. Bracher, M. Hayer-Hartl and F. Ulrich Hartl, *Annu. Rev. Biochem.*, 2013, **82**, 323-355.
61. K. Fujiwara, Y. Ishihama, K. Nakahigashi, T. Soga and H. Taguchi, *EMBO J.*, 2010, **29**, 1552-1564.
62. H. H. Kampinga and E. A. Craig, *Nat. Rev. Mol. Cell Biol.*, 2010, **11**, 579.
63. A. P. Ben-Zvi and P. Goloubinoff, *J. Struct. Biol.*, 2001, **135**, 84-93.
64. P. Goloubinoff, A. Mogk, A. P. B. Zvi, T. Tomoyasu and B. Bukau, *Proc. Natl. Acad. Sci. U.S.A.*, 1999, **96**, 13732-13737.
65. P. I. Nikel, M. Chavarría, A. Danchin and V. de Lorenzo, *Curr. Opin. Chem. Biol.*, 2016, **34**, 20-29.
66. P. Dvořák, P. I. Nikel, J. Damborský and V. de Lorenzo, *Biotechnol. Adv.*, 2017, **35**, 845-866.
67. J. G. Linger, D. R. Vardon, M. T. Guarnieri, E. M. Karp, G. B. Hunsinger, M. A. Franden, C. W. Johnson, G. Chupka, T. J. Strathmann and P. T. Pienkos, *Proc. Natl. Acad. Sci. U.S.A.*, 2014, **111**, 12013-12018.
68. G.-Q. Chen, *Chem. Soc. Rev.*, 2009, **38**, 2434-2446.
69. A. S. Pollard, M. R. Rover and R. C. Brown, *J. Anal. Appl. Pyrolysis.*, 2012, **93**, 129-138.
70. B. Mückschel, O. Simon, J. Klebensberger, N. Graf, B. Rosche, J. Altenbuchner, J. Pfannstiel, A. Huber and B. Hauer, *Appl. Environ. Microbiol.*, 2012, **78**, 8531-8539.
71. T. N. Petersen, S. Brunak, G. von Heijne and H. Nielsen, *Nature Methods*, 2011, **8**, 785-786.
72. J. D. Bendtsen, L. Kiemer, A. Fausbøll and S. Brunak, *BMC Microbiol*, 2005, **5**, 58.
73. R. M. LoPachin and T. Gavin, *Chem. Res. Toxicol.*, 2014, **27**, 1081-1091.
74. L. N. Jayakody, J. Ferdouse, N. Hayashi and H. Kitagaki, *Crit. Rev. Biotechnol.*, 2017, **37**, 177-189.
75. A. S. Acharya and J. M. Manning, *Proc. Natl. Acad. Sci. U.S.A.*, 1983, **80**, 3590-3594.
76. R. R. Kopito, *Trends Cell Biol.*, 2000, **10**, 524-530.
77. M. Zimmer, *Chem. Rev.*, 2002, **102**, 759-782.
78. M. M. Bagdasarian, E. Amann, R. Lurz, B. Rückert and M. Bagdasarian, *Gene*, 1983, **26**, 273-282.
79. J. R. Elmore, A. Furches, G. N. Wolff, K. Gorday and A. M. Guss, *Metab. Eng. Commun.*, 2017, **5**, 1-8.
80. A. de Marco, E. Deuerling, A. Mogk, T. Tomoyasu and B. Bukau, *BMC Biotechnol*, 2007, **7**, 32.
81. G. Huijberts, T. C. de Rijk, P. de Waard and G. Eggink, *J. Bacteriol.*, 1994, **176**, 1661-1666.
82. G. Huijberts, G. Eggink, P. De Waard, G. W. Huisman and B. Witholt, *Appl. Environ. Microbiol.*, 1992, **58**, 536-544.
83. D. Salvachúa, E. M. Karp, C. T. Nimlos, D. R. Vardon and G. T. Beckham, *Green Chem.*, 2015, **17**, 4951-4967.
84. E. Martínez-García, P. I. Nikel, T. Aparicio and V. de Lorenzo, *Microb. Cell Fact.*, 2014, **13**, 159.
85. E. Martínez‐García, P. I. Nikel, M. Chavarría and V. Lorenzo, *Environmental microbiology*, 2014, **16**, 291-303.
86. J. A. de Bont, *Trends Biotechnol.*, 1998, **16**, 493-499.
87. I. Poblete-Castro, J. Becker, K. Dohnt, V. M. Dos Santos and C. Wittmann, *Appl. Microbiol. Biotechnol.*, 2012, **93**, 2279-2290.
88. P. I. Nikel, M. Chavarría, A. Danchin and V. de Lorenzo, *Curr. Opin. Chem. Biol.*, 2016, **34**, 20-29.
89. D. C. Elliott, G. G. Neuenschwander, M. R. Phelps, T. R. Hart, A. H. Zacher and L. J. Silva, *Ind. Eng. Chem. Res.*, 1999, **38**, 879-883.
90. D. C. Elliott, T. R. Hart and G. G. Neuenschwander, *Ind. Eng. Chem. Res.*, 2006, **45**, 3776-3781.
91. J. M. Skerker, D. Leon, M. N. Price, J. S. Mar, D. R. Tarjan, K. M. Wetmore, A. M. Deutschbauer, J. K. Baumohl, S. Bauer and A. B. Ibánez, *Mol. Syst. Biol.*, 2013, **9**, 674.
92. C. A. Tomas, N. E. Welker and E. T. Papoutsakis, *Appl. Environ. Microbiol.*, 2003, **69**, 4951-4965.
93. C. Desmond, G. Fitzgerald, C. Stanton and R. Ross, *Appl. Environ. Microbiol.*, 2004, **70**, 5929-5936.
94. A. A. Dominguez, W. A. Lim and L. S. Qi, *Nature reviews Molecular cell biology*, 2016, **17**, 5.
95. A. B. Biter, S. Lee, N. Sung and F. T. Tsai, *Proc. Natl. Acad. Sci. U.S.A.*, 2012, **109**, 12515-12520.
96. M. Ask, V. Mapelli, H. Höck, L. Olsson and M. Bettiga, *Microb. Cell Fact.*, 2013, **12**, 87.
97. G. Richarme, C. Liu, M. Mihoub, J. Abdallah, T. Leger, N. Joly, J.-C. Liebart, U. V. Jurkunas, M. Nadal and P. Bouloc, *Science*, 2017, eaag1095.
98. J. G. Hengstler, J. Fuchs, S. Gebhard and F. Oesch, *Mutat. Res.*, 1994, **304**, 229-234.
99. M.-Z. Xie, M. I. Shoulkamy, A. M. Salem, S. Oba, M. Goda, T. Nakano and H. Ide, *Mutat. Res.*, 2016, **786**, 41-51.
100. Y. Guan, R. C. Manuel, A. S. Arvai, S. S. Parikh, C. D. Mol, J. H. Miller, R. S. Lloyd and J. A. Tainer, *Nat. Struct. Mol. Biol.*, 1998, **5**, 1058-1064.
101. T. Lindahl, *Nature*, 1993, **362**, 709-715.
102. E. Papouli, S. Chen, A. A. Davies, D. Huttner, L. Krejci, P. Sung and H. D. Ulrich, *Mol. Cell*, 2005, **19**, 123-133.
103. S. Bergink and S. Jentsch, *Nature*, 2009, **458**, 461-467.
104. E. Markkanen, B. van Loon, E. Ferrari, J. L. Parsons, G. L. Dianov and U. Hübscher, *Proc. Natl. Acad. Sci. U.S.A.*, 2012, **109**, 437-442.
105. M. O. Sommer, G. M. Church and G. Dantas, *Mol. Syst. Biol.*, 2010, **6**, 360.
106. M. T. Guarnieri, M. A. Franden, C. W. Johnson and G. T. Beckham, *Metab. Eng. Commun.*, 2017, **4**, 22-28.
107. M. A. Franden, L. Jayakody, W.-J. Li, N. J. Wagner, B. Hauer, L. M. Blank, N. Wierckx, J. Klebensberger and G. T. Beckham, *Metab. Eng.*, **In revision**
108. J. J. Schauer, M. J. Kleeman, G. R. Cass and B. R. Simoneit, *Environ. Sci. Technol.*, 2001, **35**, 1716-1728.
109. V. Shingler, F. C. H. Franklin, M. Tsuda, D. Holroyd and M. Bagdasarian, *Microbiology*, 1989, **135**, 1083-1092.
110. I. Poblete-Castro, D. Binger, A. Rodrigues, J. Becker, V. A. M. dos Santos and C. Wittmann, *Metab. Eng.*, 2013, **15**, 113-123.
111. Q. Liu, G. Luo, X. R. Zhou and G.-Q. Chen, *Metab. Eng.*, 2011, **13**, 11-17.
112. F. Velázquez, K. Pflüger, I. Cases, L. I. De Eugenio and V. de Lorenzo, *J. Bacteriol.*, 2007, **189**, 4529-4533.
113. C. W. Johnson, P. E. Abraham, J. G. Linger, P. Khanna, R. L. Hettich and G. T. Beckham, *Metab. Eng. Commun.*, 2017.
114. C. W. Johnson, D. Salvachúa, P. Khanna, H. Smith, D. J. Peterson and G. T. Beckham, *Metabolic Engineering Communications*, 2016, **3**, 111-119.

115. D. R. Vardon, M. A. Franden, C. W. Johnson, E. M. Karp, M. T. Guarnieri, J. G. Linger, M. J. Salm, T. J. Strathmann and G. T. Beckham, *Energy Environ. Sci*, 2015, **8**, 617-628.
116. T. Polen, M. Spelberg and M. Bott, *J. Bacteriol.*, 2013, **167**, 75-84.
117. M. D. Lynch and R. T. Gill, *Biotechnol. Bioeng.*, 2006, **94**, 151-158.
118. A. Shäfer, A. Tauch, W. Jäger, J. Kalinowski, G. Tierbach and A. Pühler, *Gene*, 1994, **145**, 69-73.
119. K.-H. Choi, A. Kumar and H. P. Schweizer, *J. Microbiol. Methods.*, 2006, **64**, 391-397.
120. I. Blomfield, V. Vaughn, R. Rest and B. Eisenstein, *Mol. Microbiol.*, 1991, **5**, 1447-1457.
121. C. W. Johnson and G. T. Beckham, *Metab. Eng.*, 2015, **28**, 240-247.
122. J. Monod, *Annu Rev Microbiol.*, 1949, **3**, 371-394.
123. R. A. Fisher, in *Breakthroughs in Statistics*, Springer, 1992, pp. 66-70.
124. J. Zar, *Am. J. Cardiol.*, 1979, **43**, 1159.

Graphic abstract for table of contents:

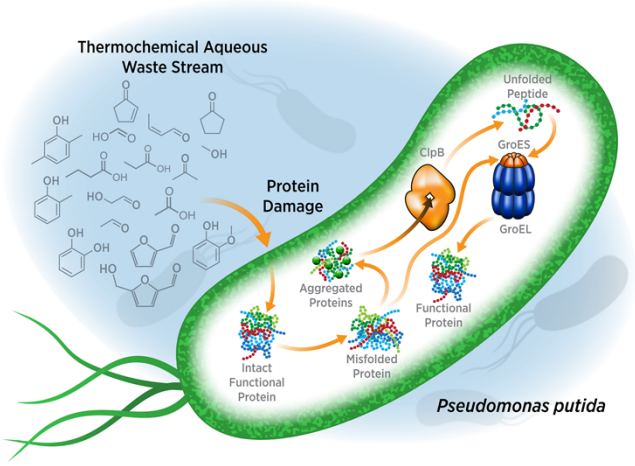

Engineering *Pseudomonas putida* for enhanced protein quality control machinery improves its toxicity tolerance, enabling biological valorization of thermochemical wastewater streams.